Published in final edited form as:
J Biol Chem. 2005 January 21; 280(3): 2002–2011. doi:10.1074/jbc.M406509200.

Structure-Activity Relationships of Diastereomeric Lysine Ring Size Analogs of the Antimicrobial Peptide Gramicidin S:

MECHANISM OF ACTION AND DISCRIMINATION BETWEEN BACTERIAL AND ANIMAL CELL MEMBRANES*

Elmar J. Prenner[‡,§], **Monika Kiricsi**[‡,¶], **Masood Jelokhani-Niaraki**[‡,‖], **Ruthven N. A. H. Lewis**[‡], **Robert S. Hodges**[‡,**], and **Ronald N. McElhaney**[‡,‡‡]

[‡]Department of Biochemistry and Protein Engineering Network of the Centers of Excellence, University of Alberta, Edmonton, Alberta T6G 2H7, Canada

[**]Department of Biochemistry and Molecular Genetics, University of Colorado Health Sciences Center at Fitzsimons, Aurora, Colorado 80045

Abstract

Structure-activity relationships were examined in seven gramicidin S analogs in which the ring-expanded analog GS14 [cyclo-(VKLKV*d*YPLKVKL*d*YP)] is modified by enantiomeric inversions of its lysine residues. The conformation, amphiphilicity, and self-association propensity of these peptides were investigated by circular dichroism spectroscopy and reversed phase high performance liquid chromatography. ^{31}P nuclear magnetic resonance spectroscopic and dye leakage experiments were performed to evaluate the capacity of these peptides to induce inverse nonlamellar phases in, and to permeabilize phospholipid bilayers; their growth inhibitory activity against the cell wall-less mollicute *Acholeplasma laidlawii* B was also examined. The amount and stability of β-sheet structure, effective hydrophobicity, propensity for self-association in water, ability to disrupt the organization of phospholipid bilayers, and ability to inhibit *A. laidlawii* B growth are strongly correlated with the facial amphiphilicity of these GS14 analogs. Also, the magnitude of the parameters segregate these peptides into three groups, consisting of GS14, the four single inversion analogs, and the two multiple inversion analogs. The capacity of these peptides to differentiate between bacterial and animal cell membranes exhibits a biphasic relationship with peptide amphiphilicity, suggesting that there may only be a narrow range of peptide amphiphilicity within which it is possible to achieve the dual therapeutic requirements of high antibiotic effectiveness and low hemolytic activity. These results were rationalized by considering how the physiochemical properties of these GS14 analogs are likely to be reflected in their partitioning into lipid bi-layer membranes.

The emergence of pathogenic bacteria with clinically significant resistance to conventional antibiotics is a major public health concern and provides much of the impetus for current attempts to develop newer types of clinical antibiotics that can evade bacterial drug

*This work was supported in part by operating and major equipment grants from the Canadian Institutes of Health Research (to R. N. M.), the Protein Engineering Network of Centers of Excellence (to R. N. M. and R. S. H.), and National Institutes of Health Grant R01 GM061885 (to R. S. H.).

‡‡To whom correspondence should be addressed: Dept. of Biochemistry, University of Alberta, Medical Sciences Bldg., Alberta T6G 2H7, Canada. Tel.: 780-492-2413; Fax: 780-492-0095, rmcelhan@ualberta.ca.
§Present address: Dept. of Biological Sciences, University of Calgary, Calgary, Alberta T2N 1N4, Canada.
¶Supported in part by a Hungarian Eötvös fellowship. Present address: Dept. of Biochemistry, Szeged University, Szeged H-6720, Hungary.
‖Present address: Dept. of Chemistry, Wilfrid Laurier University, Waterloo, Ontario N2L 3C5, Canada.

resistance mechanisms (1, 2). Antimicrobial peptides are among the more promising of such research candidates and are particularly attractive because they are usually part of the innate immune response of higher organisms and seem to act by degrading the barrier properties of bacterial cell membranes. Because of their nonspecific mode of action, the evolution of bacterial resistance to these agents is difficult, and these agents have thus maintained their effectiveness over evolutionary time. Unfortunately, these same properties tend to make many antimicrobial peptides unsuitable for general clinical application, mainly because of their tendency to cause hemolysis (3, 4). Consequently, much effort is currently being expended to produce antimicrobial peptides of comparable antibiotic effectiveness but with a reduced toxicity to animal cells.

Gramicidin S (GS)[1] is a cyclic decapeptide that exhibits strong antibiotic activity against a broad spectrum of Gram-negative and Gram-positive bacteria and against several pathogenic fungi (3–9). Numerous studies by us and others have shown that disruption of the barrier properties of cell membranes is the basis of the antimicrobial and hemolytic properties of GS (3, 4, 10). Thus, differential scanning calorimetry studies indicate that GS interacts more strongly with anionic than with zwitterionic phospholipid bilayers and more strongly with more fluid than with less fluid model membrane systems (11). ^{31}P NMR spectroscopy and x-ray diffraction both indicate that GS can induce inverted nonlamellar cubic phases in various phospholipid vesicles and that GS also causes the thinning of phospholipid bilayers (12, 13). Also, densitometry and sound velocimetry both indicate that GS binding to PC bilayers increases the motional freedom of the lipid hydrocarbon chains while increasing the volume compressibility and decreasing the density of its host bilayer (14). Fourier transform infrared spectroscopy also indicates that GS is located at the polar/ apolar interfacial region of phospholipid bilayers, that it penetrates more deeply into anionic and more fluid phospholipid bilayers (15), and that the presence of cholesterol attenuates the disordering effects of GS on phospholipid bilayers, primarily by reducing the penetration of the peptide into phospholipid model membranes (16). Finally, ^{19}F NMR spectroscopic studies of a ^{19}F-labeled GS analog indicate that GS is aligned with its cyclic β-sheet ring lying flat in the plane of the bilayer, as is consistent with its amphiphilic character (17). Unfortunately, because of the nonspecific basis of its action, GS is also strongly hemolytic, and its use as a clinical antibiotic is thus restricted to topical applications. However, recent work has shown that structural analogs of GS can be designed with comparable antimicrobial activity but with markedly reduced hemolytic activity (see below), suggesting the possibility that appropriate GS derivatives might be developed for use as oral or injectable broad spectrum antibiotics.

The relationship between the chemical structure of GS analogs and their antimicrobial and hemolytic activities has been the subject of numerous studies (3, 4). Unfortunately, most structural modifications of the GS molecule itself result in more or less parallel variations in antimicrobial and hemolytic activities. However, Hodges and co-workers (6–9, 18–20) have shown that the GS structural motif can be used as a platform for producing analogs that can disrupt bacterial cell membranes in preference to mammalian cell membranes. In particular they demonstrated that by varying both the size of the GS ring system and the orientation of certain amino acid side chains relative to the plane of the ring, one can obtain analogs that exhibit considerable (≥100-fold) dissociation of their antimicrobial activity from their

[1]The abbreviations used are: GS, gramicidin S, cyclo [VOL*d*FPVOL*d*FP] (the amino acid coded immediately after the *d* is the *d*-enantiomer); GS14, cyclo [VKLKV*d*YPLKVKL*d*YP]; GS14*d* K_2, cyclo [V*d*KLKV*d*YPLKVKL*d*YP]; GS14*d* cyclo [VKL*d*KV*d*YPLKVKL*d*YP]; K_4, GS14*d* K_9, cyclo [VKLKV*d*YPL*d*KVKL*d*YP]; GS14*d*K_{11}, cyclo [VKLKV*d*YPLKV*d*KL*d*YP]; GS14*d* K_2K_4, cyclo [V*d*KL*d*KV*d*YPLKVKL*d*YP]; GS14*d*K_2K_4 K_9K_{11}, cyclo [V*d*KL*d*KV*d*YPL*d*KV*d*KL*d*YP]; DPEPE, dipalmitelaidoyl phosphatidylethanolamine; LD_{50}, concentration required for 50% loss of integrity; PC, phosphatidylcholine; PE, phosphatidyleth-anolamine; POPC, 1-palmitoyl,2-oleoyl-phosphatidylcholine; POPG, 1-palmitoyl,2-oleoyl-phosphatidylglycerol; RP-HPLC, reversed phase high performance liquid chromatography; TFE, trifluoroethanol.

hemolytic properties (6–9). In fact, the more promising of such analogs (*e.g.* GS14*d*K4) usually exhibit antimicrobial activity comparable with that of GS itself but are considerably less hemolytic (8, 21). Like GS, these materials are also targeted against lipid bilayer membranes, but they exhibit an enhanced capacity to discriminate between bacterial and animal cell membranes (8, 21).

Although it is clear that lipid bilayer membranes are the primary targets of GS and its analogs (22–24), the relationships between the structural and physical properties of these molecules, their relative antimicrobial and hemolytic activities, and their capacity to discriminate between bacterial and animal cell membranes are not fully understood. To address these issues, we have examined and compared the structure-activity relationships of some GS analogs that were obtained by enantiomeric inversions of one or more of the Lys residues of GS14. These peptides have identical amino acid compositions and sequences and are well suited for this type of study because their antibiotic and hemolytic activities and their capacity to discriminate between bacterial and animal cells span a fairly broad range. We present here our studies of the conformational and amphipathic properties of these GS14 analogs, their ability to destabilize and permeabilize model lipid membranes, and their ability to inhibit the growth of the cell wall-less bacterium, *Acholeplasma laidlawii* B. We also present an evaluation of how the structural and physicochemical properties of these antimicrobial peptides are reflected in the capacity to disrupt lipid bilayer membranes and the capacity for effective discrimination between bacterial and animal cell membranes.

MATERIALS AND METHODS

GS14 and the other peptides were prepared as described previously (21). Phospholipids (Avanti Polar Lipids, Alabaster, AL) and other high purity reagents were obtained commercially and used as received. CD spectra were recorded at 25 °C using quartz cells of 0.1-cm path length with a Jasco 720 spectropolarimeter (Tokyo, Japan). Spectra were recorded using solutions containing 100 μM peptide and either buffer alone, equivolume mixtures of buffer and TFE, or buffer containing 30 mM SDS. The buffer utilized was composed of final concentrations of 10 mM Tris, 150 mM NaF, and 0.1 mM EDTA, pH 7.5.

RP-HPLC analyses were performed on a Zorbax SB-C8 column (150 × 2.1-mm inner diameter, 5 μm particle size, 300 Å pore size; Rockland Technologies, Wilmington, DE) using a Hewlett Packard 1100 chromatograph with a linear AB gradient of 0.5% B/min (solvent A: 0.05% aqueous trifluoroacetic acid, solvent B: 0.05% trifluoroacetic acid in acetonitrile) at a flow rate of 0.35 ml/min. Retention times were recorded at temperatures between 5 and 80 °C (3 °C increments) using the temperature profiling RP-HPLC protocols described previously (25).

^{31}P NMR spectra were recorded with a Bruker MSL-400 solid state spectrometer operating at 161 MHz for ^{31}P, using data acquisition and data processing protocols similar to those described previously (12). Peptide-induced leakage of calcein from POPC vesicles (diameter ~ 200 nm) was measured at 37 °C using previously published procedures (16).

A. laidlawii B was cultured in chloroform-extracted bovine serum albumin-free medium, and cell growth was monitored turbidometrically (26). The effect of the antimicrobial peptides on cell growth was monitored as a function of time after the addition of these peptides to the culture medium just before a 10% (by volume) inoculation with cells in the mid log phase of growth. Cell growth is expressed as a percentage of the maximum growth obtained in the absence of peptide.

RESULTS

Circular Dichroism Spectroscopic Studies

Illustrated in Fig. 1 are the CD spectra exhibited by GS14 and the six diasteriomeric derivatives examined. In both aqueous and membrane mimetic media, the CD spectra of GS14 exhibit large negative molar ellipticity values at wavelengths between 210 and 230 nm. This result is expected because GS14, like GS, is known to exist predominantly in an antiparallel β-sheet structure with type II β-turns (27). Over most of the range examined, GS14 exhibits molar ellipticities that are considerably greater than those of all other derivatives. Evidently, enantiomeric inversion of any of the Lys residues of GS14 causes significant distortion of the stable antiparallel β-sheet conformation that GS14 normally adopts. Also, GS14 analogs derived from single Lys inversions all exhibit higher molar ellipticity values than does GS14*d*K_2K_4, which in turn exhibits molar ellipticity values that are higher than those exhibited by GS14*d*$K_2K_4K_9K_{11}$, indicating that conformational distortions of the GS14 structure caused by enantiomeric inversion of its Lys residues increase progressively with the number of such inversions. Moreover, molar ellipticity values of the GS14 analogs derived from single Lys enantiomeric inversions decrease in the general order GS14dK_{11} ≥ GS14dK_4 > GS14dK_2 ≥ GS14dK_9, indicating that the distortions of the GS14 structure caused by the various single enantiomeric inversions are in-equivalent. Finally, the molar ellipticities of GS14*d*K_4 and GS14*d*K_{11} are generally comparable in magnitude as are those of GS14*d*K_2 and GS14*d*K_9, indicating that the conformational distortions caused by enantiomeric inversions of the K_4 and K_{11} residues of the GS14 molecule are comparable but different from those caused by enantiomeric inversions of the K_2 and K_9 residues. Thus, despite the inequivalent structures of the four single-substitution derivatives, there are some structural similarities between GS14dK_{11} and GS14dK_4 and between GS14dK_2 and GS14dK_9.

Fig. 1 also shows that all of these peptides (except GS14*d*$K_2K_4K_9K_{11}$) exhibit significantly higher molar ellipticity values when dissolved in 50 vol% TFE and in SDS-containing aqueous media than when dissolved in aqueous buffer alone. TFE-induced increases in molar ellipticity such as observed here are generally ascribed to the structure-inducing properties of that solvent (28–30). Thus, the increases in molar ellipticity values observed in TFE-containing solvents indicate that all of the peptides examined (except GS14*d*$K_2K_4K_9K_{11}$) adopt somewhat distorted conformations in aqueous media which are receptive to the structure-inducing properties of TFE. We also note that the molar ellipticity values obtained in SDS-containing aqueous media are generally comparable with those obtained in 50 vol% TFE (see Fig. 1). Such behavior is commonly observed with water-soluble amphipathic peptides that have the capacity to partition between aqueous media and lipid bilayers and are usually a reflection of the capacity for so-called inducible conformational changes in response to changes in the polarity of the local environment (see 31 and references cited therein).

RP-HPLC Studies

Under any given set of conditions, the binding of a peptide to a RP-HPLC column is determined by its intrinsic hydrophobicity, the size and spatial distribution of its hydrophobic regions, and its capacity for self-association in aqueous media (25, 32–37). Because these peptides all have the same amino acid sequences (and thus the same intrinsic hydrophobicities), retention by RP-HPLC columns is thus largely determined by facial amphiphilicity, which reflects the extent to which hydrophobic and polar residues are segregated on different faces of the molecule. The latter determines the capacity for preferential interaction with hydrophobic surfaces (when dissolved in aqueous media) and

thus provides an indirect estimate of the relative propensities of these peptides for partitioning into lipid membranes.

The RP-HPLC retention times of these peptides are summarized in Fig. 2. From these results it is evident that the facial amphiphilicity of GS14 is considerably higher than those of all other peptides. Also, the facial amphiphilicities of the four single inversion analogs are significantly higher than that of GS14*d*K_2K_4, which in turn is higher than that of GS14*d*$K_2K_4K_9K_{11}$. Moreover, the facial amphiphilicities of the single inversion analogs are all different (GS14dK_2 >GS14dK_9 >GS14dK_4 >GS14dK_{11}), and GS14*d*K_2 and GS14*d*K_9 both exhibit higher facial amphiphilicities than GS14*d*K_4 and GS14*d*K_{11}. Thus, the facial amphiphilicities of these derivatives decrease markedly as the number of enantio-meric inversions increases. Moreover, single enantiomeric in-versions at the K_2 and K_9, and at the K_4 and K_{11} positions of GS14 produce compounds of comparable but distinct am-phipathic properties.

Fig. 2 also shows that the retention times of all peptides except GS14*d*$K_2K_4K_9K_{11}$ exhibit a biphasic response to tem-perature change. At low temperatures, retention times increase with temperature up to a maximal value beyond which further increases in temperature actually cause retention times to decrease. The GS14*d*$K_2K_4K_9K_{11}$ derivative exhibits a monotonic decrease in retention time over the entire temperature range and is the only exception to this general observation. This biphasic temperature dependence of RP-HPLC retention times has been ascribed to temperature-induced changes in the degree of hydrophobically driven self-association of peptides in aqueous media (25). These measurements thus reflect the tendencies of these peptides to self-associate in aqueous media, which reflects both their aqueous monomeric solubilities and propensities for partitioning into lipid membranes. Moreover, the maxima in the temperature profiles shown in Fig. 2 are, in effect, turning points of the monomer:oligomer equilibria of these peptides and are useful indicators of their relative propensities for self-association (25). Thus, the temperature maxima listed in Table I suggest that the self-association propensities of these peptides decreases markedly as the number of enantiomeric inversions increases (GS14 > GS14*d*K_2 ~GS14*d*K_9 >GS14*d*K4 ~ GS14*d*K_{11} >GS14*d*K_2K_4 >GS14*d*$K_2K_4K_9K_{11}$) and that the self-association propensities of GS14*d*K_2 and GS14*d*K_9 derivatives are of comparable magnitude as are those of the GS14*d*K4 and GS14*d*K_{11} analogs. Moreover, because this process is hydrophobically driven, we can also infer that the aqueous solubility of these peptides increases in the order GS14 < GS14*d*K_2 ~GS14*d*K_9 <GS14*d*K4 ~ GS14*d*K_{11} < GS14*d*K_2K_4 <GS14*d*$K_2K_4K_9K_{11}$, in the reverse order of their membrane partitioning propensities.

^{31}P NMR Spectroscopic Studies

X-ray diffraction and ^{31}P NMR spectroscopic studies both indicate that physiologically relevant GS concentrations (<4 mol%) induce the formation of inverted cubic phases in PE model membranes and in model membranes derived from total lipid extracts of bacterial membranes (12, 13, 16). It was inferred from such studies that increased lipid monolayer curvature stress is part of the mechanism whereby GS destabilizes lipid membranes. Here, ^{31}P NMR spectroscopy was used to determine whether the mode of action of these peptides is similar to GS and to evaluate whether they are likely to destabilize lipid membranes by similar mechanisms.

Illustrated in Fig. 3 are the temperature-dependent changes in the ^{31}P NMR spectra exhibited by mixtures of DPEPE with GS14 and some of the analogs studied. At temperatures below 90 °C aqueous dispersions of DPEPE alone exhibit ^{31}P NMR spectra typical of unoriented planar bilay-ers in which lipid phosphate headgroups are undergoing fast axially symmetric motion such as occurs in liquid-crystalline phospholipid bilayers (38,

39). This behavior was expected because the lamellar to inverted nonlamellar phase transition of DPEPE occurs near 92 °C (40). At low temperatures, the spectra exhibited by peptide-free and peptide-containing (4 mol%) DPEPE membranes also exhibit spectra consistent with the persistence of DPEPE bilayers. However, at high temperatures all of the DPEPE:peptide mixtures examined (except those with the GS14*d*K_2K_4 analog) exhibit ^{31}P NMR spectra that contain a sharp peak centered near 2 ppm down-field (the isotropic component), which probably arises from the formation of an inverted cubic phase (12, 13). However, as illustrated in Fig. 4, the temperature range over which this process occurs and the extent to which it takes place, vary markedly with the nature of the peptide under investigation. Thus, GS14dK_2K_4-containing DPEPE remains largely in the lamellar liquid crystalline phase until heated to above 80 °C, whereas GS14-containing DPEPE exists primary in the inverted cubic phase at all temperature above 30 °C, some 60 °C below the lamellar/inverted nonlamellar phase transition temperature of DPEPE. Also, the relative areas of the isotropic component in the ^{31}P NMR spectra decrease in the order GS14 > GS14dK_{11} >GS14dK_4 > GS14dK_2 > GS14dK_9 > GS4d$K_2K_4K_9K_{11}$ > GS14dK_2K_4 and, as observed in our CD and HPLC studies, the relative propensities of these peptides to induce cubic phase formation can be correlated with the number and position of enantiomeric inversions of Lys residues. Thus, this particular parameter is maximal with GS14 (no inversions), and it decreases markedly as the number of such inversions increases. Moreover, the four analogs derived from single enantiomeric inversions of Lys residues exhibit different propensities for inducing cubic phase formation (*i.e.* they are inequivalent), and the propensities of the GS14*d*K4 and GS14*d*K_{11} analogs are greater than those of the GS14*d*K_2 and GS14*d*K_9 derivatives. Thus, with the possibly exception of GS14dK_2K_4, these pep-tides are all capable of destabilizing lipid bilayers with respect to inverted nonlamellar structures, and variations in this property correlate well with the variations in the structural and solution properties assayed by CD and HPLC. This demonstration that GS14 and almost all of the diastereo-meric Lys analogs are capable of inducing inverted cubic phases in DPEPE also suggests that these peptides are destabilizing lipid bilayer membranes by similar mechanisms.

Permeabilization of Phospholipid Vesicles

The propensities of GS14 and its Lys diasteriomers to permeabilize phospholipid bilayers were also investigated by an examination of their capacity to release calcein entrapped in large unilamellar POPC vesicles. These studies were performed at 37 °C, well above the gel/liquid crystalline phase transition temperature of POPC, to ensure that we were determining relative degrees of peptide-induced phospholipid bilayer permeabilization in the biologically relevant lamellar liquid crystalline state. The results of these experiments are summarized in Fig. 5 as plots of relative dye leakage as a function of peptide concentration. It is clear that the extent of peptide-induced permeabilization of POPC vesicles varies significantly, and, from the apparent LD_{50} values obtained, the membrane disruptive activities of these peptides decrease in the order GS14 (~0.9 μM) > GS14*d*K_4 (~1.0 μM) > GS14*d*K_{11} (~3.0 μM) > GS14*d*K_9 (~3.7 μM) > GS14*d*K_2 (~4.0 μM) > GS14*d*$K_2K_4K_9K_{11}$ (>10 μM) > GS14dK_2K_4 (> 20 μM). The permeabilization of POPC vesicles by these peptides also correlates with the number and position of the enantiomeric inversions in a manner that is generally consistent with the results of the physical measurements presented above.

Inhibition of A. laidlawii B Growth

The effects of these peptides on the growth of *A. laidlawii* B, a cell wall-less Gram-positive bacterium (Mollicute), were also investigated to evaluate the relationship between the physical measure-ments on GS14 and its analogs described above and their antimicrobial properties. *A. laidlawii* B is ideally suited for this type of work because the composition, organization, and dynamics of its membrane lipid bilayer have been studied extensively (41,

42) and because the absence of a cell wall or outer membrane should allow these peptides to interact directly with its cell membrane lipid bilayer, the presumed primary target of this class of antimicrobial peptides (3, 4, 10). It has been suggested that the lipopolysaccharides in the cell wall or outer membrane of Gram-negative bacteria and the lipopeptidoglycan outer layer of Gram-positive bacteria may compete for the binding of antimicrobial peptides with the lipid bilayer of the inner membrane or physically exclude the peptides from the periplasmic space (24). Our use of *A. laidlawii* B to assay the antibiotic potencies of these peptides is thus intended to circumvent some of the problems involved in studying conventional walled bacteria.

The effects of GS14 and its analogs on *A. laidlawii* B growth (see Fig. 6) indicate quite clearly that considerable variation in the growth inhibitory potency of these peptides exists. Thus, GS14 exhibits significant inhibition of *A. laidlawii* growth at peptide concentrations near 0.2 μM with complete inhibition occurring at peptide concentrations near and above 0.5 μM, whereas with GS14*d*$K_2K_4K_9K_{11}$, there was no discernible in-hibition of *A. laidlawii* B growth at peptide concentrations up to 20 μM. Enantiomeric inversions of the Lys residues of GS14 markedly diminish the growth inhibitory potencies of these peptides and, as observed in the physical measurements above, the magnitude of this effect seems to be generally correlated with the number and positions of the Lys enantiomeric inversions made. Thus growth inhibition by GS14 (no inversions, apparent LD_{50} ~0.2 μM) is significantly greater than that of the single inversion derivatives GS14*d*K_2, GS14*d*K_4, GS14*d*K_9, and GS14*d*K_{11} (apparent LD_{50} values 1–3 μM), which in turn greatly exceeds those of the multiple inversion analogs GS14*d*K_2K_4 and GS14*d*$K_2K_4K_9K_{11}$ (apparent LD_{50} values >20 μM). Also, as with the other studies reported here, the growth inhibitory potencies of the four single inversion analogs differ (*i.e.* they are inequivalent), but in this case there does not appear to be a clear segregation of these analogs into the two subgroups identified in the physical measurements.

The therapeutic indices of these compounds against *A. laid-lawii* B are presented in Fig. 7*A* as plots of therapeutic index as a function of the RP-HPLC retention time. These therapeutic indices are the ratios of the LD_{50} values required for hemolytic and antibiotic activity and are thus useful gauges of the relative capacities of these peptides to discriminate between bacterial cells and erythrocytes. In this case, the therapeutic indices calculated decrease in the order GS14*d*K_4 ≫ GS14*d*K_{11} ≫ GS14*d*K_9 > GS14*d*K_2 ≫ GS14*d*K2K_4 > GS14*d*$K_2K_4K_9K_{11}$ ≫ GS14, and unlike all other parameters examined here, there appears to be a more complex relationship between the therapeutic indices and the structural properties of these molecules. Thus, as illustrated in Fig. 7*A*, the therapeutic indices exhibit a biphasic relationship with peptide facial amphilicity, in marked contrast to the hemolytic and antibiotic activities from which they are derived (Fig. 7*B*). However, it is also clear that changes in antibiotic activity *per se* are too small to account for the magnitudes of some of the therapeutic indices calculated. Thus, the changes in the therapeutic indices and, by inference, the capacity to discriminate between animal and bacterial cell membranes, occur largely because the structural modifications of the GS14 molecule have a proportionally greater effect on the hemolytic activities of these peptides (Fig. 7*B*). A similar pattern of behavior was reported in studies of other analogs of GS14 (6, 8, 18, 19). The possible basis of these and other aspects of the behavior of these peptides are explored under “Discussion.”

DISCUSSION

The data presented in this and previous studies of the physical properties of these peptides and of their interactions with model and biological membranes are summarized in Table II. Regardless of technique used, the magnitude of the parameters measured suggests that these peptides can be segregated into three groups. At one extreme is GS14, the peptide that is, by

far, the most highly structured, the most amphiphilic, the most effective at inducing nonlamellar phases in DPEPE bilayers, the most effective at permeabilizing POPC vesicles, and the most potent inhibitor of *A. laidlawii* growth. At the other extreme is a group consisting of the two multiple inversion analogs (GS14*d*K_2K_4 and GS14*d*$K_2K_4K_9K_{11}$), which exhibit the least structure, the lowest amphiphilicity, the weakest antimicrobial activity, and are the least effective at perturbing lipid membranes. Each of the single inversion analogs has unique properties, and they form a group with physical, antibiotic, hemolytic, and general membrane disruptive properties in between these two extremes; they seem to be behaving as two nonoverlapping subgroups of closely related compounds (*viz*. GS14*d*K_2 and GS14*d*K_9, and GS14*d*K_4 and GS14*d*K_{11}). More-over, although not as active at disruptping lipid membranes as GS14, these compounds seem to have a greater capacity to discriminate between bacterial and animal cell membranes, and the GS14*d*K_4 and GS14*d*K_{11} pair is the most effective in this regard (8).

Before suggesting possible molecular explanations for these data, we shall examine the structure of the GS14 molecule to evaluate how its properties are likely to be affected by enantiomeric inversions of one or more of its Lys residues. GS14 is a cyclic tetradecamer consisting of two antiparallel aligned *β*-sheets of alternating hydrophobic and cationic residues (VKLKV and LKVKL) connected by type II′ *β*-turns composed of *d*YP (8, 27). GS14 thus forms a fairly rigid, highly amphipathic structure in which the polar and hydrophobic residues are completely segregated on opposite faces of the molecule, and the two antiparallel *β*-sheet segments are stabilized by four cross-ring hydrogen bonds (see Fig. 8). Molecular models show that the amide protons and carbonyl groups of its hydrophobic Val and Leu residues are all oriented inward, facilitating the formation of cross-ring hydrogen bonds, whereas the amide protons and carbonyl groups of the polar Lys residues all point outward from the ring and cannot form intramolecular hydrogen bonds. Also, the C_α protons of the Lys residues are all oriented inward across the ring, unlike those of the Val and Leu residues, which are directed outward away from the center of the ring. The inward orientation of the Lys C_α protons is particularly significant because enantiomeric inversions these l-Lys residues will replace the C_α protons with charged bulky Lys side chains and vice versa. However, because of the greater size of the Lys side chains, this change in orientation will be sterically unfavorable and will destabilize the *β*-sheet conformation of GS14. Reorientation of these Lys side chains will also change the charge distribution on the surface of the molecule, thereby decreasing its amphipathicity. Enantiomeric inversions of the Lys residues of GS14 can thus be expected to produce derivatives with amphipathic properties and backbone conformations that differ markedly from that of GS14, which in turn will be reflected in their solution properties, their interactions with hydrophobic surfaces, and their capacity to partition into and modulate the properties of lipid membranes (see below). Indeed, these predictions have been confirmed by studies demonstrating that enantiomeric inversion of the K_4 residue of GS14 disrupts the cross-ring hydrogen bonding network present in GS14 and produces a derivative with an altered backbone conformation, attenuated amphipathicity, and markedly different propensities for binding to and perturbing lipid bilayer membranes (20–23).

Unlike GS, GS14 has an asymmetric amino acid sequence, and there are thus chemical inequivalences that are relevant to this work. The polar face of GS14 contains the four pseudosym-metrically located, positively charged amino groups of its K_2, K_4, K_9 and K_{11} side chains (Fig. 8). These Lys residues are chemically inequivalent and give rise to unique, well resolved amide proton resonances in high resolution ^{1}H NMR spectra (8). However, there are similarities in the LKV*d*Y and VKL*d*Y sequences enveloping the K_4 and K_{11} residues, respectively, and in the PVKL and PLKV sequences enveloping the K_2 and K_9 residues, respectively. Also, the K_4 and K_{11} side chains are close enough to the *d*Y_6 and *d*Y_{13} residues, respectively, for contacts between the positively charged amino groups and

the *β*-electrons of the tyrosine residues, whereas such contacts are unlikely for the amino groups on the K_2 and K_9 side chains. Because of these structural features, there are similarities between the local environments of the K_2 and K_9 residues of GS14 and between those of the K_4 and K_{11} residues. Thus, although the four diastereomers obtained by single enantiomeric inversions of the Lys residues of GS14 are inequivalent, the properties of diastereomers formed through inversions at K_2 and K_9 are relatively similar, as are the properties of the diastereomers formed by inversions at K_4 and K_{11}.

These structural considerations provide a natural basis for explaining many aspects of the behavior of these peptides as reported by us and others (8) and in particular, the various groups and subgroups alluded to above. A general feature of the data is that the physicochemical properties of the diastereomeric derivatives deviate progressively from those of GS14 as single and multiple enantiomeric inversions of its Lys residues are made. For example, our CD results indicate that the conformation of GS14 contains considerably more *β*-sheet structure than single inversion derivatives such as GS14*d*K_4, which in turn are richer in *β*-sheet structure than the multiple inversion derivatives GS14*d*K_2K_4 and GS14*d*$K_2K_4K_9K_{11}$. The CD data follow naturally from the structural features of GS14, from which one would expect that enantiomeric inversions of one or more of its Lys residues will produce derivatives with backbone conformations that are quite distorted from the stable *β*-sheet conformation of GS14 and that progressively greater distortions of this stable conformation would occur as multiple enantiomeric Lys inversions are made. This underlying theme persists in all of the physical measurements of the peptides in solution and in virtually all of our assays of the effects of these peptides on the properties of both model and natural lipid membranes. Moreover, consistent with the chemical inequivalence of the four Lys residues of GS14 and the similarities in the chemical environments of the K_2 and K_9 and the K_4 and K_{11} residues, each of the four diastereomers obtained by single enantiomeric inversions of the Lys residues of GS14 behaves as a unique entity as regards their physicochemical properties and their interaction with lipid bilayer membranes, but they seem to form two nonoverlapping groups of closely related compounds.

Although most of the data presented here are consistent with the structural correlations discussed above, there is one obvious but possibly revealing exception. When assayed against Gram-negative and Gram-positive bacteria, the antibiotic activity of GS14 is very weak and in fact, considerably weaker than that of any of the single inversion analogs examined here (8). This result is incongruous with our results, which indicate that GS14 perturbs model lipid membranes very strongly and is a strong inhibitor of *A. laidlawii* B growth. However, it has been suggested that the weak antimicrobial activity of GS14 against Gram-negative bacteria may be attributable to its binding preferentially to the negatively charged lipopolysaccharides in the cell walls of those organisms (7, 24). This suggestion is supported by studies showing that the affinity of GS14 for lipopolysaccharide is at least an order of magnitude greater than those of the other diastereomers examined (8). The possibility that interaction of membrane-targeted antimicrobial peptides and other antimicrobial agents with negatively charged components of bacterial cell walls may essentially mask their inherent capacity to perturb bacterial membranes is not usually considered in studies such as these.

The structural properties of GS14 and analogs may also provide some insight into the probable basis of the membrane disruptive activities of these peptides. Molecular models show that when oriented with the ring plane parallel to the bilayer surface, GS14 projects onto a membrane surface an excluded cross-sectional area of some 230–300$Å^2$. However, in this orientation, its hydrophobic length along the bilayer normal is considerably shorter than the hydrophobic thickness of lipid monolayers present on the outer surfaces of natural cell membranes. Thus, if GS14 partitions into the polar/apolar interfaces of lipid bilayers and is

oriented with its ring plane parallel to the membrane surface (its most probable location and orientation (17)), it will probably laterally displace some 6–8 lipid molecules. However, because of the considerable mismatch between its hydrophobic length and the hydrophobic thickness of the host monolayer, there will be considerable packing and curvature strain on the membrane because the hydrophobic volume of GS14 would be insufficient to compensate for the combined hydrophobic volumes of the lipid molecules displaced. Thus, on the basis of simple geometric considerations alone, one can infer that the accumulation of significant amounts of GS14 in any cell membrane is inherently incompatible with the maintenance of a stable bilayer with viable barrier function, aside from any other effects that these molecules may have. Moreover, because it is unlikely that enantiomeric inversions of the lysine residues of GS14 will drastically diminish its overall molecular dimensions, one can also infer that the accumulation of significant amounts of any of these diastereomeric derivatives in cell membranes is also inherently incompatible with viable cell membrane function. The suggestion that these structurally related diastereomeric peptides are all inherently highly disruptive of normal membrane function has a number of interesting implications regarding the possible basis of the wide variations in their antibiotic, hemolytic, and other membrane disruptive activities (see below).

The structural observations noted above provide a natural basis for explaining why molecules such as GS14 can be so highly disruptive of membrane function. However, by themselves, they do not explain the wide variations in the degree of membrane disruptive behavior exhibited by these cyclic diastereomeric derivatives, especially when one considers that the amino acid compositions and sequences of these peptides are identical and that they probably disrupt lipid membranes by similar mechanisms (see ^{31}P NMR data). However, a possible explanation for this is suggested by the RP-HPLC data, which clearly show that these enantiomeric inversions of the Lys residues of GS14 markedly alter the facial amphiphilicities of these peptides. As noted earlier, facial amphiphilicity is a reflection of the capacity for preferential interaction with hydrophobic surfaces and thus provides an indirect estimate of the relative propensities for partitioning into lipid membranes. It is thus possible that the variations in peptide-induced disruption of both model and natural lipid membranes reported by us and others (8) may be largely attributable to differences in the amounts of these peptides which actually partition into membranes under comparable conditions. This possibility is supported by the results of this and previous studies showing that changes in the membrane partitioning propensities of GS14 and these diastereomeric derivatives (as inferred from HPLC retention times) are positively correlated with changes in their antibiotic and hemolytic activities (Fig. 7*B*; Refs. 6, 8, 18–20). However, the data also show that the correlation between these parameters is not perfect, which implies that there may be other influences superimposed upon the effects attributable to the differential partitioning of these peptides into lipid membranes. The latter could be indicative of subsidiary effects arising from variations in the innate membrane disruptive propensities of the individual peptides.

The suggestion that the membrane disruptive activities exhibited by these peptides are largely a reflection of the quantities that actually partition into lipid membranes also implies that differential partitioning into bacterial and animal cell membranes is a major factor involved in their capacity to discriminate between bacterial and animal cell membranes. In turn, this implies that differences between the bulk physicochemical properties of bacterial and animal cell membranes, and more specifically between the properties of their polar/apolar interfacial regions (the presumed location of these peptides in lipid membranes), are the primary basis for their capacity to discriminate between the two types of membranes. This possibility is one of the hypotheses guiding current attempts at the rational design of therapeutically useful antimicrobial peptides (44, 45), and our studies of GS and its analogs are consistent with this premise (16, 23).[2] A comparison of the lipid compositions of

bacterial and erythrocyte membranes indicates that the main compositional differences between these naturally occurring membranes are that the outer surfaces of erythrocyte membranes are composed of predominantly zwitterionic phospholipids and substantial amounts of cholesterol, whereas the outer surfaces of bacterial membranes are devoid of cholesterol and contain significant amounts (~20–40 mol%) of negatively charged phospholipids (43, 46). Our studies of GS14*d*K4 (the derivative with the highest therapeutic index) indicate that the apparent LD_{50} value for dye release from POPG vesicles is comparable with that reported here for POPC vesicles, but some 10–20-fold-lower than that required for dye release from cholesterol-rich POPC vesicles,[3] and our Fourier transform infrared spectroscopic studies indicate that such behavior is the result of poor GS14*d*K4 partitioning into cholesterol-rich PC bilayers (23).[2]

Although the hemolytic, antibiotic, and other membrane disruptive activities of these peptides are all positively correlated with membrane partitioning propensity, it is evident that the same does not to apply to the therapeutic indices (see Fig. 7). The data presented here and in studies of other GS14 analogs (6, 8, 18–20) all show a biphasic correlation between the therapeutic indices and membrane partitioning propensity in which the highest therapeutic indices do not coincide with maximal antibiotic activity, and suggest that there is an optimal range of peptide amphiphilicity which is favorable to achieving high selectivity. These results are not easily explained by the structural considerations discussed above but can be rationalized on the basis of their differential partitioning into membranes as follows. With peptides such as GS14*d*$K_2K_4K_9K_{11}$ and GS14*d*K_2K_4, their antibiotic and hemolytic activities are both very weak largely because of poor partitioning into membranes over the concentration ranges tested, and the low therapeutic indices are merely a reflection of this fact. At the other extreme are peptides such as GS14, which have a high propensity for partitioning into cell membranes, and as a result, relatively large amounts are likely to accumulate in cell membranes at all finite aqueous concentrations. For these types of peptide, the low therapeutic indices observed are probably reflecting the tendency for lethal (or at least highly injurious) quantities of these peptides to accumulate in all types of cell membrane at the concentration range usually examined. In between these two extremes are peptides such as GS14*d*K_4 (and the other single inversion analogs) whose membrane partitioning propensities are such that sub-lethal to highly injurious quantities can accumulate in cell membranes over the concentration range examined. For such molecules, discrimination between bacteria and erythrocytes will be observed if their solubility in bacterial membranes is sufficiently greater than their solubility in erythrocytes membranes to enable the existence of a nontrivial range of aqueous concentrations over which lethal amounts can accumulate in bacterial membranes but not in erythrocytes. In principle, the therapeutic indices observed in this range can be quite high, depending on intrinsic differences between the solubilities of these molecules in bacterial and animal cell membranes. However, it is implied that at least with these types of peptide, high antibiotic activity based on a high innate capacity for partitioning into lipid membranes may not be compatible with the degree of selectivity needed for therapeutic usefulness, and our data suggest that the range of peptide amphiphilicity which meets these demanding requirements may actually be rather narrow. A clearer definition of the structural and physicochemical properties of peptides or other molecules which may be compatible with these requirements is at the focus of our ongoing investigations.

[2]Abraham, T., Lewis, R. N. A. H., Hodges, R. S., and McElhaney, R. N. (2005) *Biochemistry* **44,** in press.
[3]E. J. Prenner, M. Kiricsi, T. Abraham, R. N. A. H. Lewis, R. S. Hodges, and R. N. McElhaney, unpublished experiments.

Acknowledgments

We are indebted to Drs. H. J. Vogel and D. McIntyre of the Department of Biological Sciences at the University of Calgary for the availability of instrument time and for assistance in the acquiring the ^{31}P NMR data.

References

1. Hancock RE. Lancet. 1997; 349:418–422. [PubMed: 9033483]
2. Lohner, K.; Staudegger, E. Development of Novel Antimicrobial Agents: Emerging Strategies. Lohner, K., editor. Horizon Scientific Press; Wymondham, UK: 2001. p. 149-165.
3. Izumiya, N.; Kato, T.; Aoyaga, H.; Waki, M.; Kondo, M. Synthetic Aspects of Biologically Active Cyclic Peptides: Gramicidin S and Tyrocidines. Halsted Press; New York: 1979.
4. Waki, M.; Izumiya, N. Biochemistry of Peptide Antibiotics: Recent Advances in the Biotechnology of β-Lactams and Microbial Bioactive Peptides. Kleinkaug, H.; van Doren, H., editors. Walter de Gruyter and Co; Berlin: 1990. p. 205-244.
5. Gause GG, Brazhnikova MG. Nature. 1944; 154:703.
6. Kondejewski LH, Farmer SW, Wishart D, Kay CM, Hancock RE, Hodges RS. Int J Pept Protein Res. 1996; 47:460–466. [PubMed: 8836773]
7. Kondejewski LH, Farmer SW, Wishart D, Kay CM, Hancock RE, Hodges RS. J Biol Chem. 1996; 271:25261–25268. [PubMed: 8810288]
8. Kondejewski LH, Jelokhani-Niaraki M, Farmer SW, Lix B, Kay CM, Sykes BD, Hancock RE, Hodges RS. J Biol Chem. 1999; 274:13181–13192. [PubMed: 10224074]
9. Jelokhani-Niaraki M, Kondejewski LH, Farmer SW, Hancock RE, Kay CM, Hodges RS. Biochem J. 2000; 349:747–755. [PubMed: 10903135]
10. Prenner EJ, Lewis RNAH, McElhaney RN. Biochim Biophys Acta. 1999; 1462:201–222. [PubMed: 10590309]
11. Prenner EJ, Lewis RNAH, Kondejewski LH, Hodges RS, McElhaney RN. Biochim Biophys Acta. 1999; 1417:211–223. [PubMed: 10082797]
12. Prenner EJ, Lewis RNAH, Newman KC, Gruner SM, Kondejewski LH, Hodges RS, McElhaney RN. Biochemistry. 1997; 36:7906–7916. [PubMed: 9201936]
13. Staudegger E, Prenner EJ, Kriechbaum M, Degovics G, Lewis RNAH, McElhaney RN, Lohner K. Biochim Biophys Acta. 2000; 1468:213–230. [PubMed: 11018666]
14. Krivanek R, Rybar P, Prenner EJ, McElhaney RN, Hianik T. Biochim Biophys Acta. 2000; 1510:452–463. [PubMed: 11342179]
15. Lewis RNAH, Prenner EJ, Kondejewski L, Flach CR, Mendelsohn R, Hodges RS, McElhaney RN. Biochemistry. 1999; 38:15193–15203. [PubMed: 10563802]
16. Prenner EJ, Lewis RNAH, Jelokhani-Niaraki M, Hodges RS, McElhaney RN. Biochim Biophys Acta. 2001; 1510:83–92. [PubMed: 11342149]
17. Salgado J, Grage SL, Kondejewski LH, Hodges RS, McElhaney RN, Ulrich J. J Biomol NMR. 2001; 21:191–208. [PubMed: 11775737]
18. Lee DL, Powers JPS, Pflegerl K, Vasil ML, Hancock RE, Hodges RS. J Peptide Res. 2004; 63:69–84. [PubMed: 15009528]
19. Kondejewski LH, Lee DL, Jelokhani-Niaraki M, Farmer SW, Hancock RE, Hodges RS. J Biol Chem. 2002; 277:67–74. [PubMed: 11682479]
20. Jelokhani-Niaraki M, Prenner EJ, Kondejewski LH, Kay CM, McElhaney RN, Hodges RS. J Peptide Res. 2001; 58:293–306. [PubMed: 11606214]
21. McInnes C, Kondejewski LH, Hodges RS, Sykes BD. J Biol Chem. 2000; 275:14287–14297. [PubMed: 10799508]
22. Jelokhani-Niaraki M, Prenner EJ, Kay CM, McElhaney RN, Hodges RS. J Peptide Res. 2002; 60:23–36. [PubMed: 12081624]
23. Lewis RNAH, Kiricsi M, Prenner EJ, Hodges RS, McElhaney RN. Biochemistry. 2003; 42:440–449. [PubMed: 12525171]

24. Kiricsi M, Prenner EJ, Jelokhani-Niaraki S, Lewis RNAH, Hodges RS, McElhaney RN. Eur J Biochem. 2002; 269:5911–5920. [PubMed: 12444980]
25. Lee DL, Mant CT, Hodges RS. J Biol Chem. 2003; 278:22918–22927. [PubMed: 12686558]
26. Silvius JR, McElhaney RN. Can J Biochem. 1978; 56:462–469. [PubMed: 667693]
27. Gibbs AG, Kondejewski LH, Gronwalk W, Nip AM, Hodges RS, Wishart DS. Nat Struct Biol. 1998; 5:284–288. [PubMed: 9546219]
28. Sonnichsen FD, Van Eyk JE, Hodges RS, Sykes BD. Biochemistry. 1992; 31:8790–8798. [PubMed: 1390666]
29. Blanci FJ, Jimenez MA, Pineda A, Rico M, Santoro J, Nieto JL. Biochemistry. 1994; 33:6004–6014. [PubMed: 8180228]
30. Cagas PM, Corden JL. Proteins Struct Funct Genet. 1995; 21:141–160.
31. Cornut, I.; Thiaudiere, E.; DuFourcq, J. The Amphipathic Helix. Epand, RM., editor. CRC Press; Boca Raton, FL: 1993. p. 173-219.
32. Parker JMR, Guo D, Hodges RS. Biochemistry. 1986; 25:5425–5432. [PubMed: 2430611]
33. Guo DC, Mant CT, Taneja AK, Parker JMR, Hodges RS. J Chromatogr. 1986; 359:499–517.
34. Wishart DS, Kondejewski LH, Semchuk PD, Sykes BD, Hodges RS. Lett Peptide Sci. 1996; 3:53–60.
35. Mant CT, Zhou NE, Hodges RS. J Chromatogr. 1989; 476:363–375. [PubMed: 2777984]
36. Rothemund S, Krause E, Beyermann M, Dathe M, Bienert M, Hodges RS, Sykes BD, Sonnichsen FD. Peptide Res. 1996; 9:79–87. [PubMed: 8738982]
37. Krause E, Beyermann M, Fabian H, Dathe M, Rothemund S, Bienert M. Int J Peptide Res. 1996; 48:559–568.
38. Seelig J. Biochim Biophys Acta. 1978; 515:105–140. [PubMed: 356883]
39. Campbell RF, Meirovitch FE, Freed JH. J Phys Chem. 1979; 83:525–533.
40. Silvius JR, Lyons M, Yeagle PL, O'Leary TJ. Biochemistry. 1985; 24:5388–5395. [PubMed: 4074703]
41. Smith, PF. Mycoplasmas: Molecular Biology and Pathogenesis. Maniloff, J.; McElhaney, RN.; Finch, LR.; Baseman, JB., editors. American Society for Microbiology; Washington, D. C: 1992. p. 79-91.
42. McElhaney, RN. Mycoplasmas: Molecular Biology and Pathogenesis. Maniloff, J.; McElhaney, RN.; Finch, LR.; Baseman, JB., editors. American Society for Microbiology; Washington, D. C: 1992. p. 113-155.
43. Nes, WR.; McKern, ML. Biochemistry of Steroids and Other Isoprenoids. University Park Press; Baltimore, MD: 1977.
44. Matsuzaki K, Sugishita K, Fujii N, Miyajima K. Biochemistry. 1995; 34:3423–3429. [PubMed: 7533538]
45. Tytler EM, Anantharamaiah GM, Walk DE, Mishra VK, Palgunachari MN, Segrest JP. Biochemistry. 1995; 34:4393–4401. [PubMed: 7703253]
46. Yeagle, PL. The Biology of Cholesterol. Yeagle, PL., editor. CRC Press; Boca Raton, FL: 1988. p. 121-145.

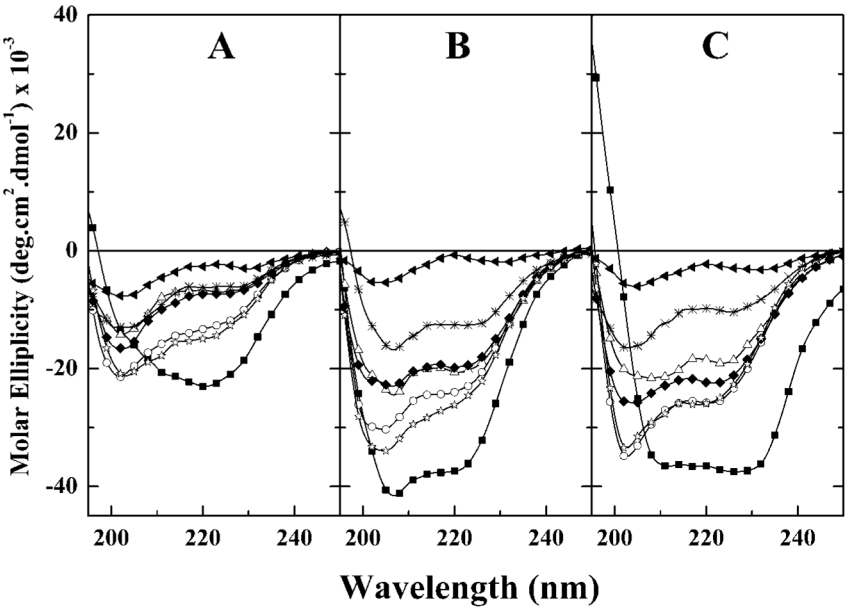

Fig. 1. CD spectra of GS14 and its diastereomeric derivatives dissolved in aqueous solution (*A*), 50% TFE (*B*), and in SDS-containing aqueous media (*C*)

The spectra shown are representative of GS14 (■), GS14*d*K_2(△), GS14*d* K_4 (○), GS14*d* K_9 (◆),GS14*d* K_{11} (☆), GS14*d* K_2K_4 (*), and GS14*d*. $K_2K_4K_9K_{11}$ (▲)

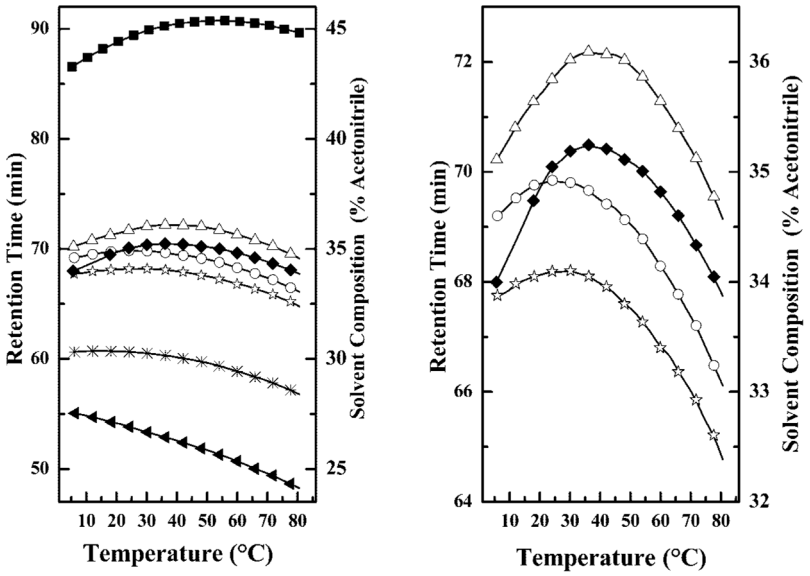

Fig. 2. Effect of temperature on the retention times of GS14 and its di-astereomeric analogs on a RP-HPLC column

The temperature profiling curves of the four diastereomers obtained by single enantiomeric inversions of the Lys residues of GS14 are shown on an expanded scale in the *right panel*. Data are presented for GS14 (■), GS14*d* K_2(△), GS14*d* K_4 (○), GS14*d*K_9 (◆), GS14*d* K_{11} (☆) GS14*d*K_2K_4 (*), and GS14*d*$K_2K_4K_9K_{11}$ (▲)

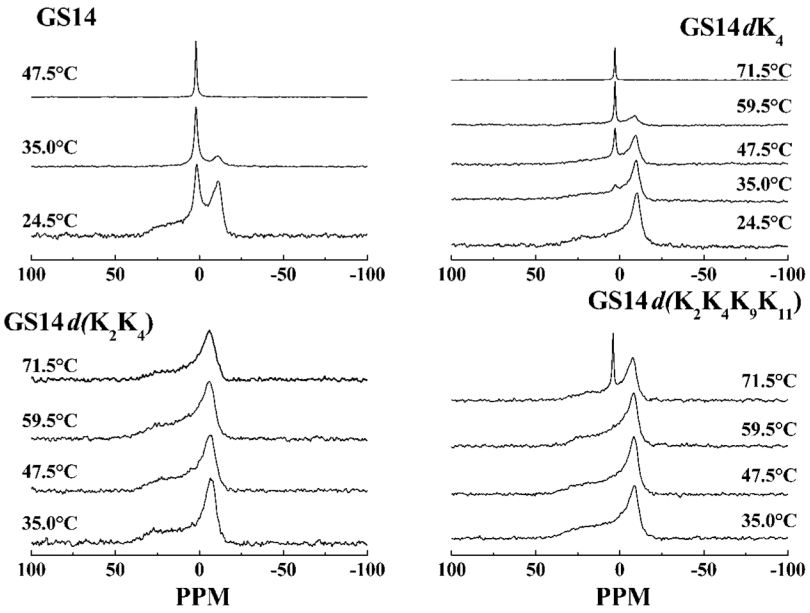

Fig. 3. Proton-decoupled ^{31}P NMR powder patterns exhibited by mixtures of GS14 and some of its dia-stereomeric Lys derivatives with DPEPE

The spectra shown were acquired at the temperatures indicated using mixtures with an overall lipid: peptide ratio of 25:1.

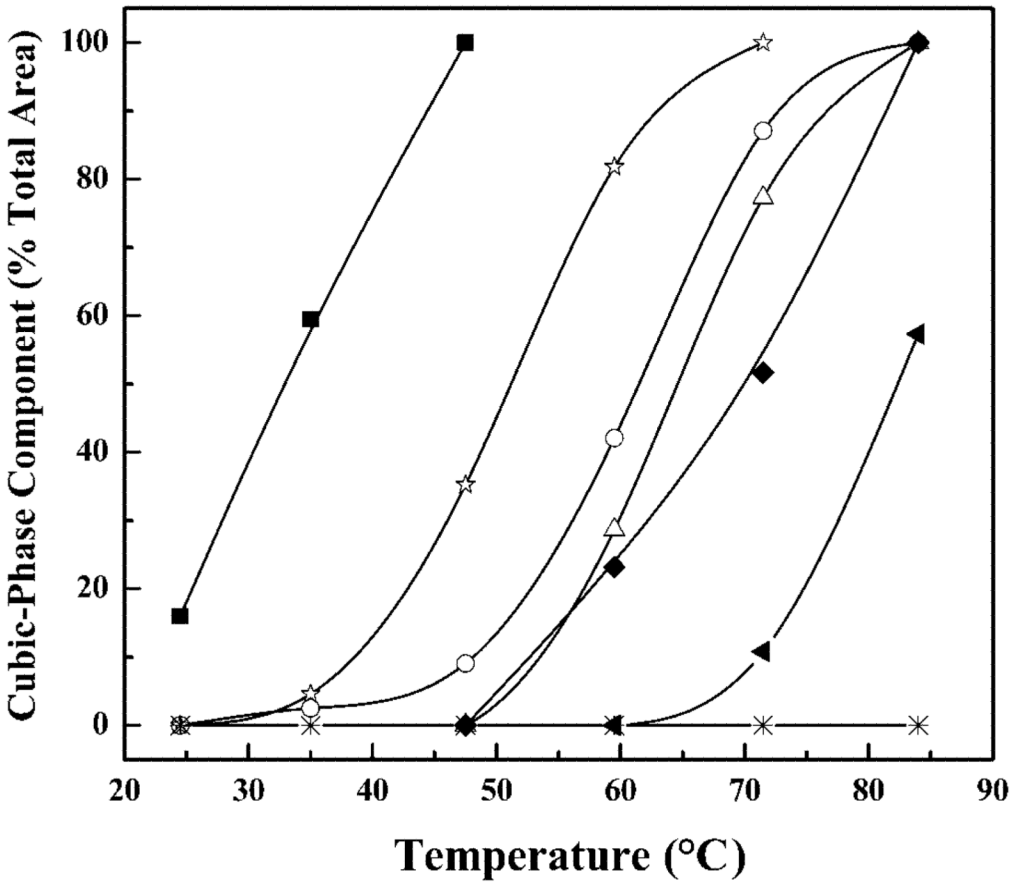

Fig. 4. Temperature-dependent changes in the relative areas of the isotropic peak (~2 ppm downfield) in the ^{31}P NMR spectra exhibited by DPEPE mixtures with GS14 and the various diaste-reomeric Lys derivatives studied

Data are presented for GS14 (■), GS14*d* K_2(△), GS14*d* K_4 (○), GS14*d* K_9 (◆), GS14*d* K_{11} (☆), GS14*d* K_2K_4 (*), and GS14*d* $K_2K_4K_9K_{11}$ (▲)

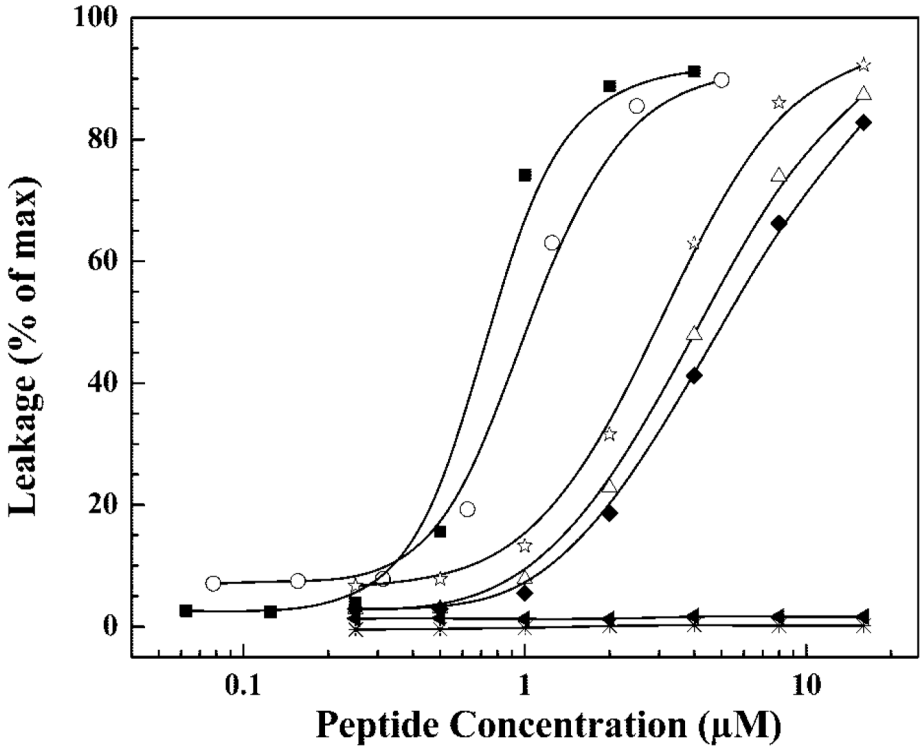

Fig. 5. Peptide induced dye release from large unilamellar POPC vesicles

Data are presented as a function of peptide concentration for the following peptides: GS14 ((■), GS14*d* K_2 (△), GS14*d*K_4(○), GS14*d* K_9 (◆), GS14*d* K_{11} (☆), GS14*d* K_2K_4 (*), and GS14*d*. $K_2K_4K_9K_{11}$(▲)

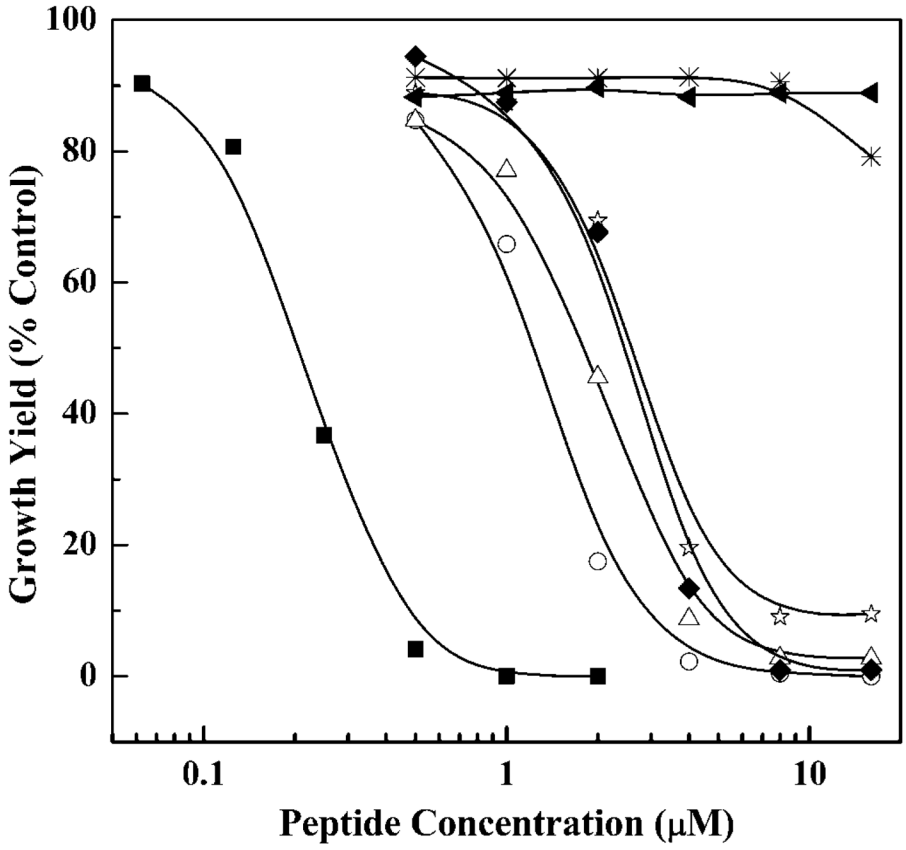

Fig. 6. Effect of GS14 and its diastereomeric analogs on the growth of *A. laidlawii* B

Data are presented as a function of peptide concentration for the following peptides: GS14 (■), GS14*d*K_2 (△), GS14*d*K_4 (○), GS14*d*K_9 (◆), GS14*d*K_{11} (☆), GS14*d*K_2K_4 (*), and GS14*d*$K_2K_4K_9K_{11}$ (▲).

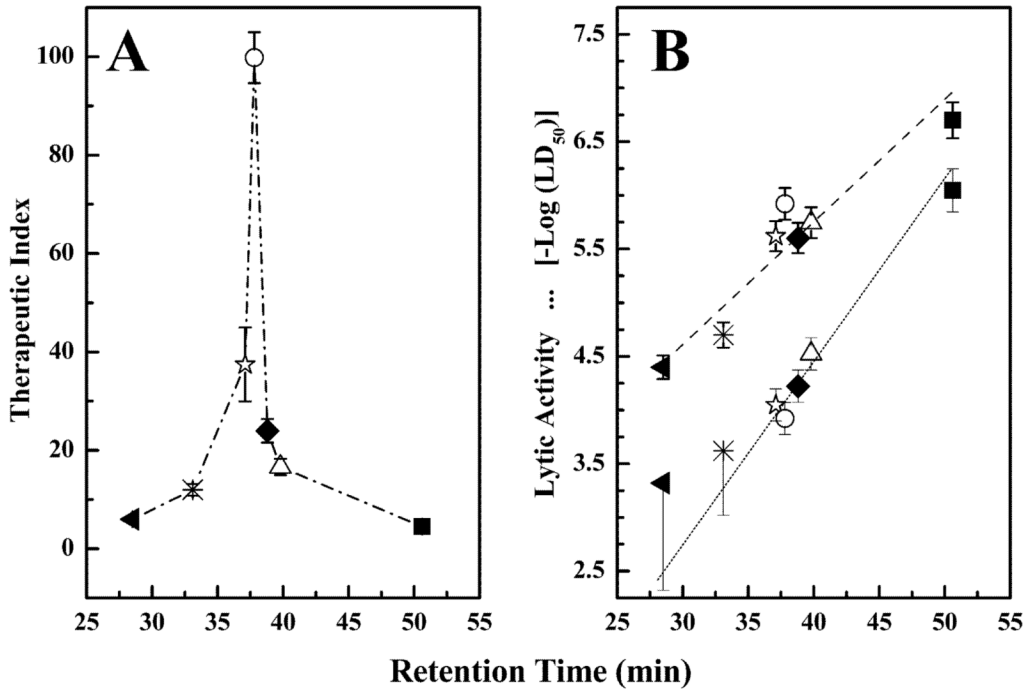

Fig. 7. Plots of the therapeutic indices (*A*) and the antibiotic (*B, upper line*) and hemolytic activities (*B, lower line*) of GS14 and its lysine diastereomers as a function of the retention times of the peptides on a RP-HPLC column

Antibiotic activities were measured against *A. laidlawii* B and are expressed as the negative logarithm of the apparent LD_{50} values determined from the data presented in Fig. 6. The hemolytic activity data were obtained from Ref. 8. The therapeutic indices are the ratios between the apparent LD_{50} values for inhibition of *A. laidlawii* B growth and the hemolytic activity and are thus a gauge of the capacity of these peptides to discriminate between *A. laidlawii* B cells and erythrocytes. The *symbols* represent data points obtained with the following peptides: GS14 (■), GS14*d*K_2 (△), GS14*d*K_4 (○), GS14*d*K_9 (◆), GS14*d*K_{11} (☆), GS14*d*K_2K_4 (*), and GS14*d*$K_2K_4K_9K_{11}$ (▲).

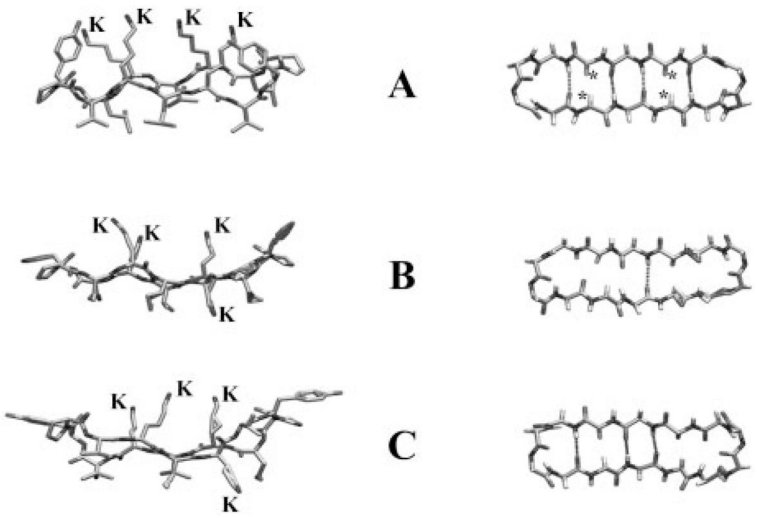

Fig. 8. Molecular models of the antibiotic peptides GS14 (*A*) and GS14-*d*K_4 (*B* and *C*)

The *left images* show side views of the peptide backbone and the orientations of the Lys (*K*) and hydrophobic (unlabeled) side chains relative to the ring plane. The *right images* show top views of the peptide backbone with the * *symbols* marking the positions of the inward oriented Lys C_α protons of GS14 and the *dashed lines* representing connectivities where the distance and orientation of the amide carbonyls and amide protons are favorable for cross-ring hydrogen bonding. The GS14 model shown was obtained from minimized structures published by Gibbs *et al.* (27), and the GS14-*d*K_4 models were obtained from the NMR solution structures in water (*B*) and 30% TFE (*C*) determined by McInnes *et al.* (21).

Table I

Temperature maxima of the retention times of GS14 and its lysine diastereomeric derivatives on a reversed phase HPLC column

Peptide sample[a]	Temperature maximum
	°C
GS14	54.2
GS14*d* K_2	38.7
GS14*d* K_9	38.4
GS14*d* K_4	26.1
GS14*d* K_{11}	26.1
GS14*d* K_2K_4	14.6
GS14*d* $K_2K_4K_9K_{11}$	<5

[a] Sorted in decreasing order of retention times.

Table II

Comparison of the assayed properties of GS14 and its diastereomeric analogs

Assayed property	As deduced from	Ranking order	Ref.
β-Sheet content in H_2O	CD	GS14 ≫ dK$_{11}$ > dK$_4$ > dK$_9$ > dK$_2$ ≫ dK$_2$K$_4$ > dK$_2$K$_4$K$_9$K$_{11}$	This work
β-Sheet content in membrane mimetic media	CD	GS14 ≫ dK$_{11}$ > dK$_4$ > dK$_9$ ≥ dK$_2$ ≫ dK$_2$K$_4$ > dK$_2$K$_4$K$_9$K$_{11}$	This work
Facial amphiphilicity	RP-HPLC	GS14 ≫ dK$_2$ > dK$_9$ > dK$_4$ > dK$_{11}$ ≫ dK$_2$K$_4$ > dK$_2$K$_4$K$_9$K$_{11}$	This work
Self-association	RP-HPLC	GS14 ≫ dK$_2$ > dK$_9$ > dK$_4$ > dK$_{11}$ ≫ dK$_2$K$_4$ > dK$_2$K$_4$K$_9$K$_{11}$	This work
Aqueous solubility	RP-HPLC	dK$_2$K$_4$K$_9$K$_{11}$ ≫ dK$_2$ K$_4$ ≫ dK$_{11}$ > dK$_4$ > dK$_9$ > dK$_2$ > GS14	This work
Cubic phase induction	^{31}P NMR	GS14 ≫ dK$_{11}$ > dK$_4$ > dK$_2$ > dK$_9$ ≫ dK$_2$K$_4$K$_9$K$_{11}$ > dK$_2$K$_4$	This work
Membrane lysis	Calcein dye leakage from POPC vesicles	GS14 ≫ dK$_4$ > dK$_{11}$ > dK$_2$ > dK$_9$ ≫ dK$_2$K$_4$ > dK$_2$K$_4$K$_9$K$_{11}$	This work
LPS binding affinity	Dansyl polymixin B displacement	GS14 ≫ dK$_2$ ~ dK$_{11}$ > dK$_9$ > dK$_4$ ≫ dK$_2$K$_4$ > dK$_2$K$_4$K$_9$K$_{11}$	8
Antibiotic activity	*A. laidlawii* B	GS14 ≫ dK$_4$ > dK$_2$ > dK$_{11}$ ~ dK$_9$ ≫ dK$_2$K$_4$ > dK$_2$K$_4$K$_9$K$_{11}$	This work
Antibiotic activity	Gram-negative bacteria	dK$_4$ > dK$_{11}$ > dK$_9$ > dK$_2$ ≫ dK$_2$K$_4$ > GS14 ~ dK$_2$K$_4$K$_9$K$_{11}$	8
Antibiotic activity	Gram-positive bacteria	dK$_{11}$ > dK$_4$ > dK$_9$ > dK$_2$ ≫ GS14 ≫ dK$_2$K$_4$ > dK$_2$K$_4$K$_9$K$_{11}$	8
Antibiotic activity	Fungal growth	GS14 > dK$_{11}$ ~ dK$_2$ > dK$_4$ ~ dK$_9$ > dK$_2$K$_4$ > dK$_2$K$_4$K$_9$K$_{11}$	8
Hemolytic activity	Human erythrocyte lysis	GS14 ≫ dK$_2$ > dK$_9$ > dK$_{11}$ > dK$_4$ ≫ dK$_2$K$_4$ > dK$_2$K$_4$K$_9$K$_{11}$	8
Therapeutic indices	Hemolytic, antifungal, and antibacterial activities	dK$_4$ > dK$_{11}$ ≫ dK$_9$ > dK$_2$ ≫ dK$_2$K$_4$ > dK$_2$K$_4$K$_9$K$_{11}$ ≫ GS14	8